



Novel benzoxazole inhibitors of mPGES-1

Natasha Kablaoui^a, Snahel Patel^b, Jay Shao^a, Douglas Demian^c, Keith Hoffmaster^d, Francoise Berlioz^e, Michael L. Vazquez^f, William M. Moore^g, Richard A. Nugent^{a,*}

^a Pfizer Research Technology Center, 620 Memorial Dr., Cambridge, MA 02139, USA

^b Genentech Inc., 1 DNA Way, South San Francisco, CA 94080, USA

^c Blue Sky Biotech, Inc., 60 Prescott St., Worcester, MA 01605, USA

^d Novartis Inc., 250 Massachusetts Ave., Cambridge, MA 02139, USA

^e Vertex, 130 Waverly St., Cambridge, MA 02139, USA

^f Pfizer Global Research, 445 Eastern Point Road, Groton, CT 06340, USA

^g Monsanto Company, 800 N. Lindbergh Blvd., St. Louis, MO 63167, USA

ARTICLE INFO

Article history:

Received 20 June 2012

Revised 2 October 2012

Accepted 8 October 2012

Available online 16 October 2012

Keywords:

mPGES-1

Benzoxazole

Selective

ABSTRACT

A novel series of potent benzoxazole mPGES-1 inhibitors has been derived from a hit from a high throughput screen. Compound **37** displays mPGES-1 inhibition in an enzyme assay (0.018 μM) and PGE-2 inhibition in a cell-based assay (0.034 μM). It demonstrates 500- and 2500-fold selectivity for mPGES-1 over COX-2 and 6-keto PGF-1 α , respectively. In vivo PK studies in dogs demonstrate 55% oral bioavailability and an 7 h half-life.

© 2012 Elsevier Ltd. All rights reserved.

For patients with inflammatory pain caused by osteoarthritis (OA) and rheumatoid arthritis (RA), the first line of treatment is nonsteroidal anti-inflammatory drugs (NSAIDs) and COX-2 inhibitors (COXIBs). The COXIBs are superior to NSAIDs due to their lower incidence of gastrointestinal side effects, but they have shown renal toxicity and increased cardiovascular risk.¹ Alternate mechanisms for treating inflammatory pain may address some of the shortfalls of the current first line treatments.

Prostaglandin E₂ (PGE₂) is an inflammatory mediator that plays a central role in controlling pain and swelling, and is found in the synovial fluid of patients with OA and RA.^{2,3} The biosynthesis of PGE₂ begins with the cleavage of arachidonic acid (AA) from membrane phospholipids by phospholipase A₂, followed by the conversion of AA to PGH₂ by cyclooxygenase (COX), and finally to the production of PGE₂ by PGE synthase (PGES).⁴ Three forms of PGES have been reported: cytosolic PGES (cPGES), microsomal PGES-1 (mPGES-1), and microsomal PGES-2 (mPGES-2).⁴ Both cPGES and mPGES-2 are constitutively expressed in a variety of tissues, while mPGES-1 is up-regulated under inflammatory conditions.^{2,4,5} Synthesis of excessive PGE₂ at inflammatory sites is caused by the up-regulation of COX-2 and mPGES-1 in response to inflammatory mediators. An inhibitor of mPGES-1 would be expected to inhibit

up-regulated PGE₂ synthesis associated with inflammatory disorders while sparing constitutive PGE₂, prostacyclin (PGI₂), and thromboxane (TXA₂) production for GI, renal, and cardiovascular homeostasis.

There are several reported small molecule mPGES-1 inhibitors in the literature (Fig. 1). MK-886, **1**,⁶ an indole-based 5-lipoxygenase-activating protein (FLAP) inhibitor (IC₅₀ = 0.026–0.1 μM), displays mPGES-1 inhibition for rat (IC₅₀ = 8.2 μM) and human (IC₅₀ = 1.6 μM). Merck-Frosst scientists have reported on several inhibitor classes, including **2**,⁷ which is structurally similar to MK-886. Compound **2** is a potent and selective mPGES-1 inhibitor (IC₅₀ = 0.003 μM) on the recombinant human mPGES-1 enzyme, but a 2000-fold shift was observed for PGE₂ inhibition in a IL-1 β stimulated A549 whole cell. More recently Merck-Frosst has disclosed MF63 **3**,⁸ a non-acidic, phenanthreneimidazole, which bears no structural resemblance to previous inhibitors, but is highly active (IC₅₀ = 0.001 μM).⁹ The trisubstituted urea **4**¹⁰ has also been shown to be a selective and powerful inhibitor (IC₅₀ = 0.001 μM). Pfizer has shown that biaryl oxicams, such as **5**,¹¹ are selective inhibitors of mPGES-1 (IC₅₀ = 0.016 μM), but are highly protein bound. Herein we report a new series of potent and selective benzoxazole mPGES-1 inhibitors, which are efficacious in cellular assays and are orally bioavailable in dogs.

Screening of the Pfizer compound collection identified **6** as a modest inhibitor of human mPGES-1, with an IC₅₀ = 1.2 μM (Fig. 2). Examination of other, related benzoxazoles through

* Corresponding author.

E-mail address: richardnugent@flatleydiscoverylab.com (R.A. Nugent).

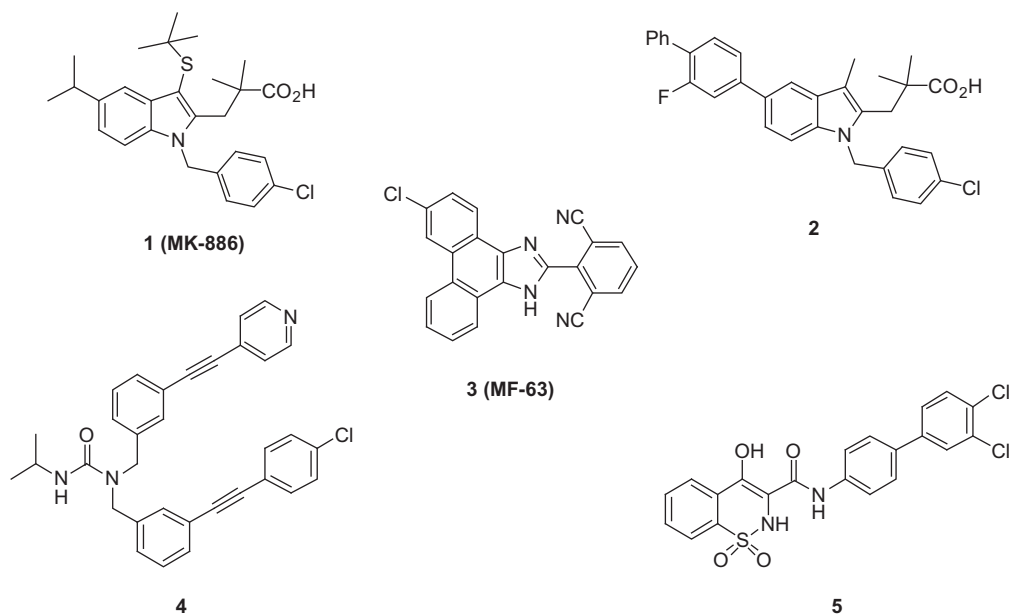


Figure 1. Previously reported mPGES-1 inhibitors.

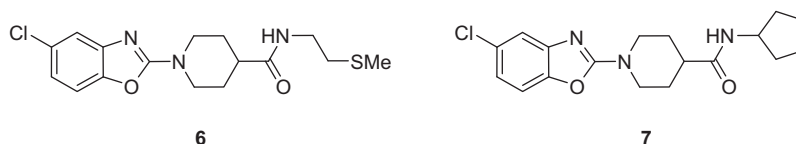


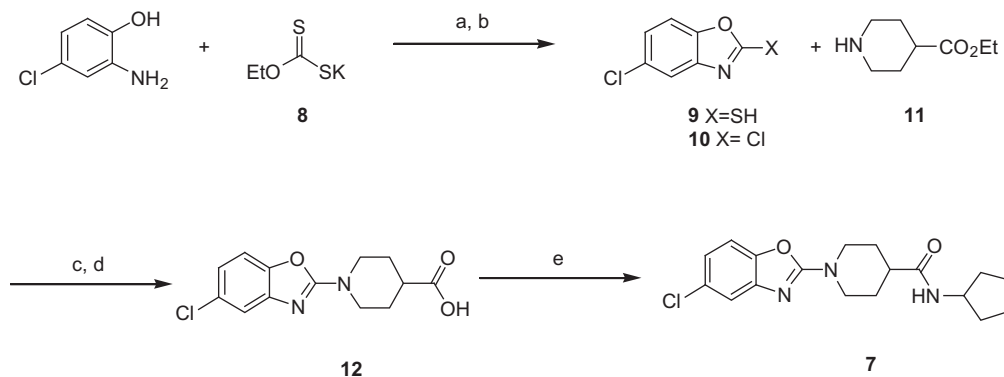
Figure 2. Lead compounds from HTS screening.

similarity and substructure searching of the Pfizer collection led to the discovery of **7**, which has increased potency ($IC_{50} = 0.85 \mu\text{M}$) and selectivity for mPGES-1 (PGE_2) over COX-2 ($PGF_{2\alpha}$) in an IL-1 stimulated fetal fibroblast cell assay¹² (PGE_2 $IC_{50} = 1.01 \mu\text{M}$; $PGF_{2\alpha}$ $IC_{50} > 100 \mu\text{M}$). Compound **7** offers several positive attributes, including low molecular weight and $clogP$, which allow significant changes to the structure without destroying its drug-like character. Compound **7** is stable to human liver microsomes and is predicted by the Pampa assay¹³ to have high permeability; a drawback is that it displays high protein binding (99.5%), which negatively impacts its efficacy in whole blood assays.

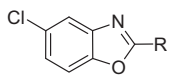
Analogs were synthesized according to Scheme 1, which details the synthesis of compound **7**. Commercially available 2-amino-4-chloro phenol and **8** are heated in refluxing pyridine for 1 h; work up gives crude thiol **9** in 90% yield. Without purification, **9**

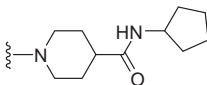
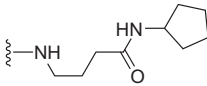
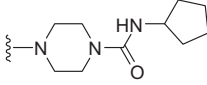
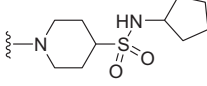
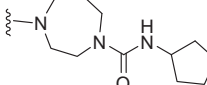
is dissolved in DCM, cooled to 0°C , then treated with chlorine gas until the solid dissolves. The reaction is warmed to rt, and stirred for 4 h, at which time HPLC shows complete consumption of starting material. After workup, **10** is isolated in 87% yield. Next, **10** and the ester **11** are dissolved in DCM, treated with triethylamine, and stirred at rt for 2 h. The solvent is evaporated and the residue dissolved with MeOH/water, followed by hydrolysis of the ester with NaOH to give **12** in 99% yield. Treatment of **12** with cyclopentylamine, HBTU, and triethylamine in DMF completes the synthesis of **7**. Overall yields are typically $>80\%$.

Compound **7** is a very modular structure, and the general synthetic scheme allows for a systematic examination of the contributions of the various motifs to mPGES potency and physical properties. Tables 1–3 illustrate the effects on mPGES inhibitory activity of modifications to the piperidine, the amide linker, and



Scheme 1. Reagents and conditions: (a) pyridine, reflux, 90%; (b) Cl_2 (g), DCM, 87%; (c) Et_3N , DCM; (d) MeOH/ H_2O (9:1), NaOH; (e) cyclopentylamine, HBTU, Et_3N , DMF.

Table 1
SAR of mPGES-1 inhibition by varying linker shape


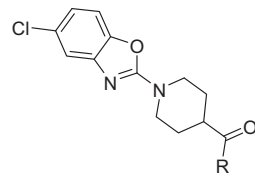
	R	mPGES-1 IC ₅₀ (μM)
7		0.853
13		>10
14		>10
15		>10
16		12.9

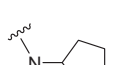
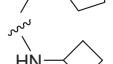
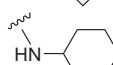
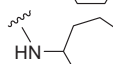
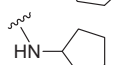
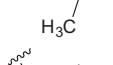
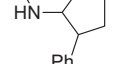
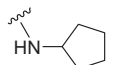
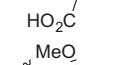
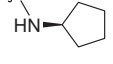
the amide substituent, while holding the 4-chloro benzoxazole constant. The modifications to the piperidine and amide linker are not tolerated, but changes to the amide substituent improve mPGES potency and physical properties.

Modifications to the piperidine and amide functionality are shown in Table 1. Compounds **13–16** are synthesized by treating **10** with the appropriate amine as described above. Simple modifications to this region are not tolerated. For example, opening the piperidine ring, **13**, or replacing it with a piperazine, **14**, results in loss of all activity. The homopiperazine, **16**, has measurable inhibition, but it is very weak. The sulfonamide **15** is also inactive.

The amide substituent is a more fruitful area for improving mPGES activity through structural modifications. Parallel synthesis of analogs **19–37** is accomplished as described in Scheme 2. Compound **17** and amines **18a–m** are dissolved in DMF and treated with triethylamine and HBTU and stirred overnight. After workup, the crude material is treated with 1 M HCl in MeOH, and finally with **10** and triethylamine in DMF. The resulting material is purified by reverse phase HPLC to yield the desired compound in >95% purity.

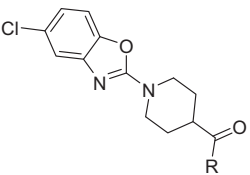
Table 2 details changes in ring size and substitution pattern of the amide. A dramatic loss of activity is observed when the secondary amide of **7** is replaced with the tertiary amide, **19**. Changes to the ring size of the amide substituent does not play a significant role in activity, as there is only a modest improvement in potency as the ring size increases from four to seven carbons, **20–22**. This is likely due to increased lipophilicity, as measured by the steady increase of *clogP*. Derivatization of the cyclopentyl ring, **23–25** also demonstrates a similar improvement in potency with increased lipophilicity. Comparison of compounds **23** and **24**, with a methyl and phenyl ring in the 2-position, respectively, shows no difference in potency despite the much larger phenyl ring in **24**; this suggests that there may be a large, hydrophobic pocket near the amide nitrogen. Ethers **26–28** have increasingly large substituents in that 2-position, probing this space. While potency for these compounds still tracks with lipophilicity, compounds **27** and **28** (IC₅₀ = 0.826 and 0.176 μM, respectively) show that the presumed pocket is large and flexible. The amines necessary to synthesize these compounds are accessible through a procedure described by BASF^{14,15}

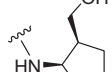
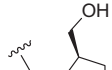
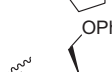
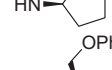
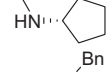
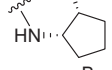
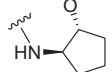
Table 2
Survey of novel amides


Compd	R	<i>cLogP</i>	mPGES IC ₅₀ (μM)
7		2.65	0.853
19		2.92	>30
20		2.09	3.01
21		3.21	1.68
22		3.76	0.821
23		3.16	0.242
24		4.20	0.291
25		2.11	7.18
26		2.46	8.15
27		3.90	0.826
28		4.41	0.176

and can be modified to provide a wide variety of 2-position substituents.

The effect of substituent chirality is explored in Table 3. Several sets of diastereomers of different ring size and lipophilicity are shown. Two diastereomer sets with low lipophilicity were examined. Serendipitously, in both the 1,4-substituted cyclohexyl example (**29/30**) and the 1,2-substituted cyclopentyl (**31/32**), the *cis* diastereomers are more active than *trans*. The other sets in Table 3 are 1,2-substituted cyclopentyl rings with higher lipophilicity (**33/34** and **35/36/37**), and no difference in activity between the diastereomers is apparent; these lipophilic compounds are also more potent, entering into the low double-digit nanomolar range. Compound **34** is also very potent in the whole cell PGES fetal fibroblast (FF) assay, but inactive in the human whole blood (HWB) assay.¹¹ The lack of whole blood activity may be due to the high PPB (>99%) measured for **34**. Compounds **35/36/37** also show a high degree of activity in the enzyme assay and FF assay, although the potency in the FF drops off for the *cis* isomer, **35**. All three compounds

Table 3
Study of *clogP* and stereochemistry


Compd	Structure	<i>clogP</i>	mPGES IC ₅₀ (μM)	FF ^b IC ₅₀ (μM)	HWB ^c IC ₅₀ (μM)
29		1.74	0.383	1.26	11.1
30		–	>19.1	>10.0	NT
31		2.05	0.785 ^a	NT	NT
32		–	3.20 ^a	NT	NT
33		4.67	0.0431	NT	NT
34		–	0.034	0.0847	>33.6
35		4.20	0.082	0.618	76.6
36		–	0.040	0.296	27.4
37		–	0.018	0.0347	7.56

^a Assay format slightly different for these compounds, with a lower amount of DMSO content.

^b FF = whole cell PGES fetal fibroblast assay.

^c HWB = human whole blood assay.¹¹

show some activity in the HWB assay, but **37** is the most potent in all three assays.

Further profiling of compound **37** is shown in Table 4. The compound is also highly protein bound, 98% in rat plasma, which explains the significant decrease in potency in the human whole blood cell assay. It is predicted to show poor permeability and is highly metabolized in rat and human microsomes with a very short

Table 4
In vitro PK assessment of **37**

Pampa Pe ($\times 10^{-6}$ cm/sec)	Rat PPB (%)	HLM <i>T</i> _{1/2} (min)	RLM <i>T</i> _{1/2} (min)
1.3	98	10.8	7.2

Table 5
In vivo PK profile of **37**

Parameter	Dog (iv)	Dog (PO) ^a
Dose (mg/kg)	0.25	0.5
Cl (mL/mg/kg)	2.1	–
MRT ^b (h)	8.1	–
<i>V</i> _{ss} (L/kg)	1.0	–
<i>C</i> _{max} (μM)	–	1.3
<i>T</i> _{1/2} (h)	7.2	–
<i>T</i> _{max} (h)	–	0.5
<i>F</i> (%)	–	55.0

^a Data is reported as mean of three animals.

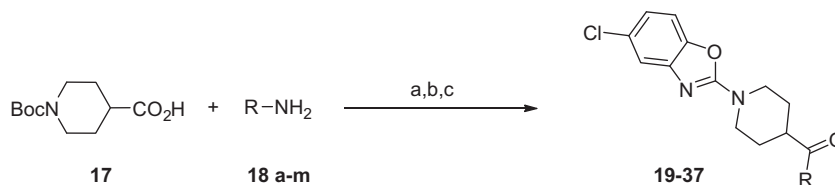
Table 6

Assay	IC ₅₀ (μM)
Human mPGES-1	0.018
Human PGDS	>10.0
IL-1 stimulated fetal fibroblast (PGE)	0.035
IL-1 stimulated fetal fibroblast with SnCl ₂ (PGF2α)	>100
Rat mPGES-1	>10
IL-1 stimulated rat synovial fibroblast assay	>30
LPS stimulated human whole blood	0.934
LPS stimulated dog whole blood	1.23

half-life in both species. However, the results of a dog PK study, shown in Table 5, belie the in vitro predictions, possibly due to differences in plasma protein binding across species. Compound **37** exhibits 55% bioavailability with a 7.2 h half-life. The high clearance predicted from rat or human liver microsomes does not predict the clearance of **37** observed in vivo in dogs. However, in vitro half-life in human hepatocytes measures 80 min, which is more in line with that observed in dogs.

Table 6 shows the inhibitory effects of compound **37** on other prostanooids. Selectivity for PGES over PGDS and PGF2 alpha is shown through enzymatic and fetal fibroblast assays, respectively. Compound **37** is not effective against rat mPGES-1, either in an enzyme assay or in IL-1 stimulated rat synovial fibroblasts,¹² demonstrating a species dependence despite the high sequence homology between human and rodent mPGES-1. This discrepancy has also been observed by Côté et al.⁸ for a phenanthrene imidazole based series of mPGES-1 inhibitors. Compound **37** does, however, show similar mPGES inhibitory activity in LPS stimulated dog and human whole blood assays.⁹

In summary, we have developed potent mPGES-1 inhibitors from a hit in a high throughput screen. These compounds demonstrate better cell activity over previously reported series.



Scheme 2. Reagents and conditions: (a) HBTU, Et₃N, DMF; (b) 1 N HCl, MeOH, 18 h; (c) **10**, Et₃N, DMF, 50 °C, 18 h.

Compound **37** displays mPGES-1 inhibition of 0.018 μM and selectivity over COX-2 in the human fetal fibroblast cell assay. It inhibits PGE₂ production in the LPS/human whole blood assay with an IC₅₀ \sim 7 μM , with the discrepancy between enzymatic and whole blood assays due to the high protein binding of the molecule. Compound **37** is well absorbed in dogs, with an unbound exposure $>3\times$ mPGES-1 IC₅₀ for 6 h following an oral dose.

Acknowledgments

The authors wish to thank Per-Johan Jakobsson of the Karolinska Institute for the development of a high throughput assay allowing the identification of the lead compounds. We also gratefully acknowledge the support and contributions of Douglas Otte, Michael Pollastri, Joan Kelly, Qing Cao, Jim Gierse, Gina Jerome, Gabriel Mbalaviele, and Alex Shaffer.

References and notes

1. Melnikova, I. *Nat. Rev. Drug Disc.* **2005**, *4*, 453.
2. Kojima, F.; Kato, S.; Kawai, S. *Fundam. Clin. Pharmacol.* **2005**, *19*, 255.
3. Futani, H.; Okayama, A.; Matsui, K.; Kashiwamura, S.; Sasaki, T.; Hada, T.; Nakanishi, K.; Tateishi, H.; Maruo, S.; Okamura, H. *J. Immunother.* **2002**, *25*, S61.
4. Park, J. Y.; Pillinger, M. H.; Abramson, R. B. *Clin. Immunol.* **2006**, *119*, 229.
5. Li, X.; Afif, H.; Cheng, S.; Martel-Pelletier, J.; Pelletier, J. P.; Ranger, P.; Fahmi, H. *J. Rheumatol.* **2005**, *32*, 887.
6. Mancini, J. A.; Blood, K.; Guay, J.; Gordon, R.; Claveau, D.; Chan, C.-C.; Riendeau, D. *J. Biol. Chem.* **2001**, *276*, 4469.
7. Riendeau, D.; Aspiotis, R.; Ethier, D.; Gareau, Y.; Grimm, E. L.; Guay, J.; Guiral, S.; Juteau, H.; Mancini, J. A.; Méthot, N.; Rubin, J.; Friesen, R. W. *Bioorg. Med. Chem. Lett.* **2005**, *15*, 3352.
8. Côté, B.; Boulet, L.; Brideau, C.; Claveau, D.; Ethier, D.; Frenette, R.; Gagnon, M.; Giroux, A.; Guay, J.; Guiral, S.; Mancini, J.; Martins, E.; Masse, F.; Methot, N.; Riendeau, D.; Rubin, J.; Xu, D.; Yu, H.; Ducharme, Y.; Friesen, R. W. *Bioorg. Med. Chem. Lett.* **2007**, *17*, 6816.
9. Xu, D.; Rowland, S. E.; Clark, P.; Giroux, A.; Côté, B.; Guiral, S.; Salem, M.; Ducharme, Y.; Friesen, R. W.; Méthot, N.; Mancini, J.; Audoly, L.; Riendeau, D. *J. Pharmacol. Exp. Ther.* **2008**, *326*, 754.
10. Chiasson, J.-F.; Boulet, L.; Brideau, C.; Chau, A.; Claveau, D.; Côté, B.; Ethier, D.; Giroux, A.; Guay, J.; Guiral, S.; Mancini, J.; Massé, F.; Méthot, N.; Riendeau, D.; Roy, P.; Rubin, J.; Xu, D.; Yu, H.; Ducharme, Y.; Friesen, R. W. *Bioorg. Med. Chem. Lett.* **2011**, *21*, 1488.
11. Wang, J.; Limburg, D.; Carter, J.; Mbalaviele, G.; Gierse, J.; Vazquez, M. *Bioorg. Med. Chem. Lett.* **2010**, *20*, 1604.
12. Mbalaviele, G.; Pauley, A.; Shaffer, A.; Zweifel, B.; Mathialagan, S.; Mnich, S.; Nemirovskiy, O.; Carter, J.; Gierse, J.; Wang, J.; Vazquez, M.; Moore, W.; Masferrer, J. *Biochem. Pharmacol.* **2010**, *79*, 1445.
13. Kansy, M.; Senner, F.; Gubernator, K. *J. Med. Chem.* **1998**, *41*, 1007.
14. Siegel, W.; Haderlein, G.; Staeb, T. PCT Int. Appl., WO 2007 074047, 2007; *Chem. Abstr.* **147**, 143055.
15. Govindaraju, T.; Kumar, V. A.; Ganesh, K. N. *J. Org. Chem.* **2004**, *69*, 5725.